AD-A046 597 COLORADO STATE UNIV FORT COLLINS DEPT OF CHEMISTRY F/G 7/4
RAPID SCAN ALTERNATE DROP PULSE POLAROGRAPHIC METHODS.(U)
NOV 77 J A TURNER, R A OSTERYOUNG N00014-77-C-0004
UNCLASSIFIED TR-5 NL

| OF |
ADA
046597

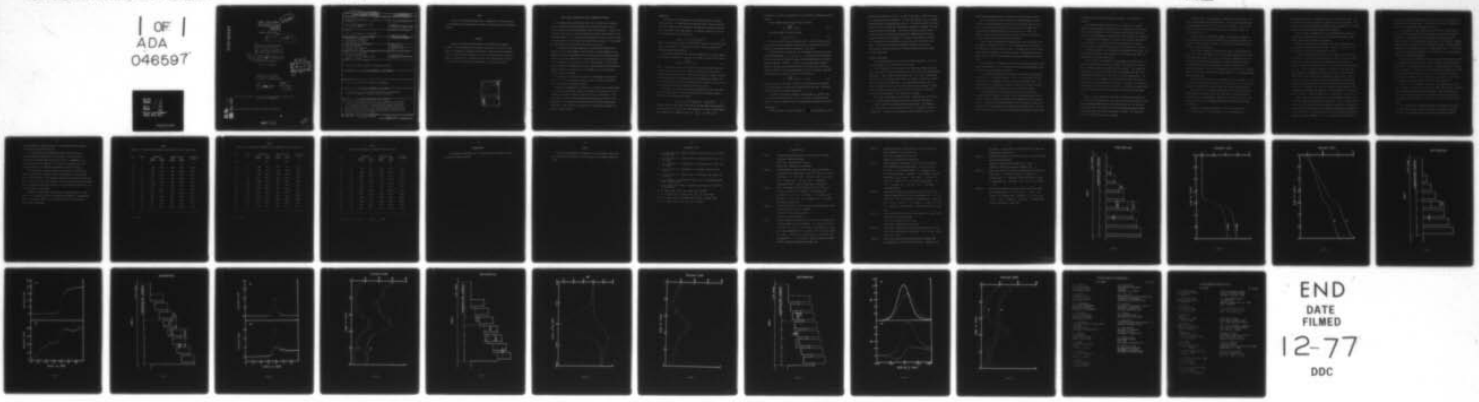

END
DATE FILMED
12-77
DDC

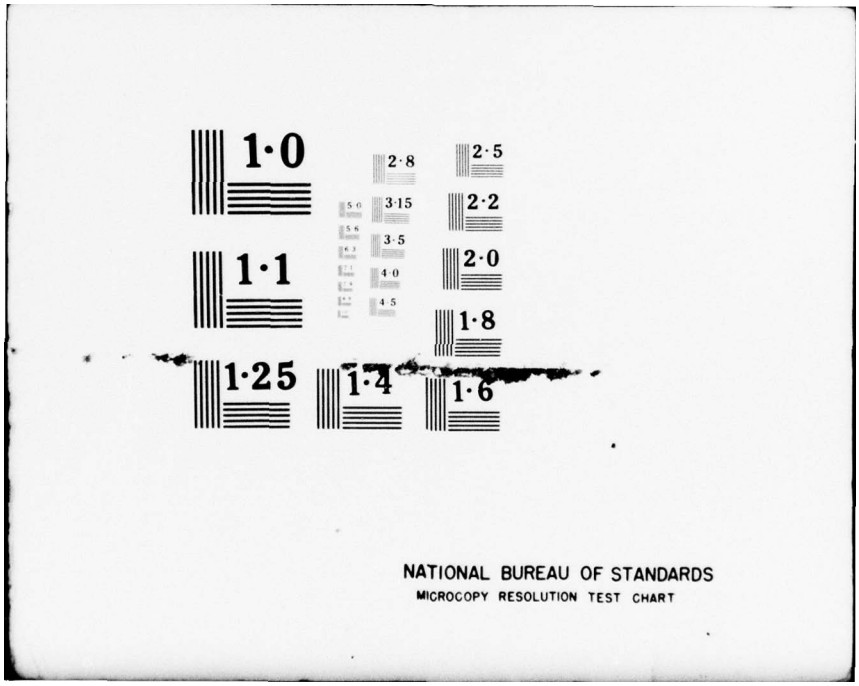
1·0
1·1
1·25
1·4
1·6
1·8
2·0
2·2
2·5
2·8
3·15
3·5
4·0
4·5
5·0
5·6
6·3
NATIONAL BUREAU OF STANDARDS
MICROCOPY RESOLUTION TEST CHART

(12) 5 p.

OFFICE OF NAVAL RESEARCH

(15) Contract N00014-77-C-0004

(14) TR-

TECHNICAL REPORT NO. 5

(9) Interim rept.,

(6) RAPID SCAN ALTERNATE DROP PULSE POLAROGRAPHIC METHODS.

by

(10) John A. Turner and R. A. Osteryoung

Prepared for Publication in

Analytical Chemistry

Department of Chemistry
Colorado State University
Fort Collins, Colorado 80523

(11) November, 1977

(12) 36p.

404992

B

Unclassified

SECURITY CLASSIFICATION OF THIS PAGE (When Data Entered)

REPORT DOCUMENTATION PAGE		READ INSTRUCTIONS BEFORE COMPLETING FORM
1. REPORT NUMBER Technical Report No. 5	2. GOVT ACCESSION NO.	3. RECIPIENT'S CATALOG NUMBER
4. TITLE (and Subtitle) Rapid Scan Alternate Drop Pulse Polarographic Methods		5. TYPE OF REPORT & PERIOD COVERED Interim 6. PERFORMING ORG. REPORT NUMBER
7. AUTHOR(s) John A. Turner and R. A. Osteryoung		8. CONTRACT OR GRANT NUMBER(s) N00014-77-C-0004
9. PERFORMING ORGANIZATION NAME AND ADDRESS Department of Chemistry Colorado State University Fort Collins, CO 80523		10. PROGRAM ELEMENT, PROJECT, TASK AREA & WORK UNIT NUMBERS
11. CONTROLLING OFFICE NAME AND ADDRESS Chemistry Program Office of Naval Research Arlington, VA 22217		12. REPORT DATE November, 1977 13. NUMBER OF PAGES 35
14. MONITORING AGENCY NAME & ADDRESS(if different from Controlling Office) Office of Naval Research Resident Representative Suite 210, 6740 E. Hampden Avenue Denver, CO 80222		15. SECURITY CLASS. (of this report) Unclassified 15a. DECLASSIFICATION/DOWNGRADING SCHEDULE

16. DISTRIBUTION STATEMENT (of this Report)

Approved for Public Release; Distribution Unlimited

17. DISTRIBUTION STATEMENT (of the abstract entered in Block 20, if different from Report)

18. SUPPLEMENTARY NOTES

Prepared for publication in Analytical Chemistry

19. KEY WORDS (Continue on reverse side if necessary and identify by block number)

differential pulse polarography; alternate drop polarography; rapid scan voltammetry; charging current compensation

20. ABSTRACT (Continue on reverse side if necessary and identify by block number)

A number of alternate drop waveforms which compensate for charging currents at the dropping mercury electrode which arise as a result of drop growth are examined in connection with several rapid scan pulse voltammetric methods. Both normal and differential pulse and square wave rapid scan waveforms are applied and it is demonstrated that the alternate drop techniques can be applied to the rapid scan methodology in an acceptable manner.

DD FORM 1 JAN 73 1473 EDITION OF 1 NOV 65 IS OBSOLETE
S/N 0102-014-6601

Unclassified

SECURITY CLASSIFICATION OF THIS PAGE (When Data Entered)

BRIEF

A number of alternate drop waveforms to compensate for charging current at the dropping mercury electrode are applied to rapid scan pulse voltammetric methods.

ABSTRACT

A number of alternate drop waveforms which compensate for charging currents at the dropping mercury electrode which arise as a result of drop growth are examined in connection with several rapid scan pulse voltammetric methods. Both normal and differential pulse and square wave rapid scan waveforms are applied and it is demonstrated that the alternate drop techniques can be applied to the rapid scan methodology in an acceptable manner.

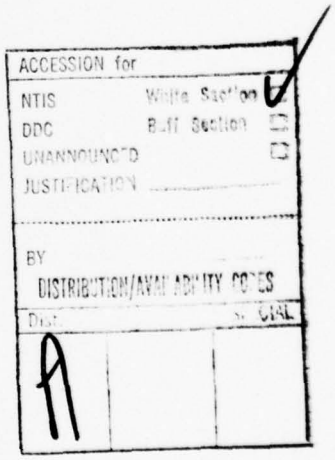

RAPID SCAN ALTERNATE DROP PULSE POLAROGRAPHIC METHODS

At a dropping mercury electrode (dme) there is added to any faradaic current a contribution from the double layer charging current, owing to the electrode area growing continuously during the experiment. Charging current must then flow at all times to maintain the proper charge density at the electrode surface. It is this charging current that limits the useful analytical concentration that the regular pulse techniques can detect. This problem has been extensively discussed by Christie et al (1,2,3,4).

The techniques that were developed to eliminate this background are based on the fact that faradaic current flowing at the dme depends on the potential and time of measurement and the past history of the waveform while the capacity current depends only on the potential and time of measurement. It is independent of the previous history of the waveform. One only then needs to make two measurements at the same time and potential with different waveform histories and subtract them to completely discriminate against charging current at the dme.

The alternate drop technique requires two measurements on successive drops (2,3). This means that the analysis time is double over standard pulse polarographic experimental methods.

Square wave voltammetry at the dme (5,6) and other rapid scanning modes (7) scan the entire potential range of interest in a single drop of a dme offering fast analysis time with little or no loss in sensitivity. They also contain as part of their background the charging current due to the growing drop. This paper will explore some rapid scanning polarographic techniques in the alternate drop mode that are designed to eliminate this type of charging current.

Theoretical

The origin of the charging current background has been thoroughly discussed (1,4). It stems from the requirement that a constant potential at a dme current must flow to maintain the appropriate surface charge density as the area of the drop changes. The charging current at any given time and potential can be given by (1)

$$I_c(E,t) = -2/3\ k\ m^{2/3}\ Q(E)/t^{1/3} \qquad (1)$$

where k is a constant (equal to .8515 $cm^2/g^{2/3}$) and Q(E) is the charge density at the potential E. The minus sign arises from the convention of cathodic current being positive.

The faradaic current for the rapid scan modes will, of course, depend on the choice of waveform; in general, the faradaic current can be given by

$$I_f(E,t) = \frac{nFACD^{\frac{1}{2}}}{\sqrt{\pi\ \tau}}\ \psi(E,t) \qquad (2)$$

where τ would be the total cycle time of the waveform, typically the time for the base staircase, and $\psi(E,t)$ would give the shape of the current potential characteristic (5,6). The explicit formation of these ψ functions could be obtained from the application of the superposition theorem (8) or the general waveform equation presented by Rifkin and Evans (9) or by use of the square wave equations presented by Christie et al (5).

If we take, for example, the square wave waveform and focus our attention on a single cycle in the train we have for the difference current a charging current contribution given by

$$\Delta I_c = -2/3\ k\ m^{2/3}\ [Q(E_1)/t_1^{1/3} - Q(E_2)/t_2^{1/3}] \qquad (3)$$

where t_1 and t_2 are the time in the life of the drop where the measurements are made [$t_2 = t_1 + \tau(\rho_2-\rho_1)$ for square wave] and E_1 and E_2 are the measurement potentials (for square wave $E_2 = E_1 - 2E_{sw}$). $\rho_1\tau$ and $\rho_2\tau$ are,

respectively, the time of measurement for the individual forward and reverse currents.

For the faradaic current alone we have as before

$$I_f = \frac{nFACD^{\frac{1}{2}}}{\sqrt{\pi}\,\tau}\,\Delta\psi(E,t) \tag{4}$$

The total current can then be written

$$\Delta I_{sw} = \Delta I_f + \Delta I_c \tag{5}$$

This is essentially the same equation that is given by Christie et al (1,2) indicating that, although the experiment is done during the life of one drop, the charging current contribution is the same.

To eliminate this contribution, one only needs to insure that for the difference measurement $t_1 = t_2$ and $E_1 = E_2$. The easiest way to accomplish this is to do scans on successive drops and make measurements at the same time and potential. However, in order to have any measurable faradaic response, one must use different waveforms for the two scans so that the faradaic response for the two measurements will not be the same. Our equation for the total faradaic current can now be given by

$$I_f = \frac{nFACD^{\frac{1}{2}}}{\sqrt{\pi}\,\tau}\,[\psi_1(E,t) - \psi_2(E,t] \tag{6}$$

where ψ_1 and ψ_2 have different potential-time characteristics but where current measurements are made at the same potential and time. The double layer charging terms now have dropped out.

To optimize the faradaic response, one would want ψ_1 to give a very large faradaic response, and ψ_2 to give a very small, or even better an opposite, faradaic response so that ΔI_f would remain as large as possible.

Experimental

A PDP-12 computer (Digital Equipment Corporation) was used for on-line

experiments and analysis of data. For some of this work, a PAR 174 was used as a potentiostat and I-E converter. For the trace analysis runs, a homemade potentiostat and I-E converter were used (7). The dropping mercury electrode assembly was the PAR Model 9337 polarography stand with a PAR Model 172A drop knocker driven by the computer. The cell was a 100 ml berzelius beaker. A saturated calomel electrode from Sargent Welch (30080-15A) with a porous platinum tip was used as reference. The counter electrode was a platinum helix separated from the solution by a pyrex tube with a pin hole in the bottom. Triple distilled mercury (Bethlehem Apparatus Co.) was used. Deaeration was done with prepurified nitrogen further purified by passage over hot copper wool.

Waveforms and Results

Each technique requires two scans with different waveforms. The first set of waveforms will be in the normal pulse vein.

The first waveform to be discussed is the rapid scan normal pulse waveform. Both type 1 and type 2 measurements (4) are possible with the alternate drop modes. Figure 1 details the waveforms used. For a type 1 measurement, the first scan is the normal pulse rapid scan waveform (solid line), measurements being made only at the pulse. The second waveform on the drop is a staircase whose potentials are coincident with the pulse potentials (dashed line); measurements are made at the same time in drop life as during the previous pulse measurement. The difference is recorded.

For a type 2 measurement, a third "scan" is made with the initial waveform. Here measurements are made just prior to the pulse application.

Figure 2 gives the current potential characteristic. The output is a rapid scan normal pulse polarogram from which is subtracted a staircase voltammogram. The waves are more drawn out than the regular rapid scan

normal pulse polarogram due to the subtraction of the staircase current.

It is fairly obvious that to optimize this mode one wants the pulse as short as possible and the delay time (time during which the drop grows prior to pulse train application) as long as possible, consummate with completing the required voltage scan during the life of a drop. The faradaic current from the staircase will then be as small as possible and will not affect the height of the wave appreciably.

Figure 3 shows an ordinary and alternate drop rapid scan normal pulse polarogram for cadmium in 0.1 M KCl. The background slope for the alternate drop mode is less but still not flat. The reason for the sloping background can be attributed to "capillary response", a phenomena discussed by Barker (10,11). The capillary response is obviously different for the two scans.

Christie et al (1,2) obtained similar results with their alternate drop normal pulse technique. It is not surprising that the same phenomena occurs with the rapid scan alternate drop modes.

It is interesting to note that although the alternate drop background is not flat, it is straight. Between -.2 and -.6 v the ordinary mode has a good deal of structure while the rapid scan mode is almost linear. Although the wave is diminished, the smaller slope and straighter background should make measurement of these waves at trace levels much easier.

The second waveform to be discussed is very similar to Christie's constant potential mode (3); the scan is just completed during the life of one drop. Figure 4 details the potential-time dependence of this waveform. For this mode pulses are always made back to the same potential (the initial potential) with the potential being stepped during the delay time. For the second "waveform" one sits at the initial potential and measures the current

at the same time the pulse measurements were made. The difference is recorded.

The faradaic response (Figure 5A) is very similar to a constant potential pulse polarogram, except the scan is completed in just two drops. If the initial potential is set so that no faradaic current flows, then there will be no diminution of the wave when the second scan is subtracted.

Figure 5B gives an example of the use of this alternate drop mode at the trace level. It is obvious that the background has been greatly decreased over the regular rapid scan normal pulse mode shown in Figure 3.

The next two modes are in the rapid scan differential pulse vein. The two waveforms have been termed differential pulse forward mode (DPF) and differential pulse reverse mode (DPR).

Figure 6 details the potential time dependence for the DPF mode. For the first scan (solid line) pulses are made in the direction of the scan with current measurements being made only at the pulse. The second scan (dashed line) is a staircase whose steps are coincident with the pulses, measurements being made at the same time as the pulse measurements. The two scans give similar faradaic responses, except near the half wave the response for the pulse measurement is greater. Thus there is a diminution involved due to the subtraction of the staircase current, the amount depending on the pulse height, step height, pulse time and delay time between pulses.

Table 1 gives calculated data for DPF for various pulse heights and pulse time to delay time ratios. This data was calculated using the square wave theoretical equations given by Christie et al (5). The diminution factor given here is the ratio of the alternate drop mode peak current to the ordinary mode peak current expressed as a percent. The larger the diminution factor, the better the response.

Of note in Table 1 is the decrease in the amount of diminution as the ratio of pulse time to delay time decreases. This is the same trend that was observed by Christie et al (1,2) for their techniques. The peak half widths are wider for the alternate drop modes but become narrower for smaller values of δ/τ.

Figure 7 gives an experimental example of the faradaic response for this technique as well as the individual pulse and staircase currents. Of interest is the tailing of the peak. This has obvious analytical implications for closely spaced peaks.

Figure 8 shows regular and alternate drop rapid scan polarograms for lead in 0.1 M KCl. The background for the alternate drop mode is not only much flatter but nearly zero. This is analytically important since it is the finite and often unknown background in ordinary differential pulse polarography that limits the usefulness of standard additions as an analytical technique. With a zero background only the criteria of linearity need be satisfied to be able to use standard additions to quantitate unknown samples at this level.

Figure 9 gives the potential-time dependence for the DPR mode. In this mode the pulses are made in the opposite direction of the scan (solid line). A staircase (dashed line) is again used as the second scanning waveform.

As a first pass, it might be expected that if the reverse pulse were large enough, the currents for the two scans would be opposite and there would be little or no diminution. However, from a perusal of Table 2, it is obvious that there is considerable diminution involved, more so than the DPF mode.

Figure 10 illustrates the problem. Much as the reverse peak is shifted with respect to the forward peak in cyclic voltammetry, so

the reverse pulse peak is shifted with respect to the staircase sweep, the reason being that the two currents are measured at the same potential. The currents are indeed opposite but unfortunately they are opposite at different potentials and thus the peak broadening and diminution.

Figure 11 gives an example of the use of DPR mode at the trace level. A comparison of this type with Figure 8 shows that DPR mode does indeed flatten and decrease the amount of background.

Although the peak widths for DPR mode are slightly narrower, there is less diminution involved with the DPF mode. The exact usefulness of each will naturally depend on the experimental situation.

The final alternate drop waveform to be discussed utilizes the square wave waveform. The essence of this technique is that it involves scanning two successive drops with square wave waveforms which are shifted by π relative to each other and which differ in their relative initial potentials by 2 E_{sw}. Figure 12 gives the waveform and timing. For the first scan, only forward pulse measurements are made (solid line); the second scan involves taking only reverse pulse measurements (dashed line). This is virtually identical to a regular square wave experiment except here the forward and reverse currents are measured at the same potential and time in the life of the drop. For the figure shown here the waveforms for the two sweeps have complementary symmetries. If the symmetry of the forward pulse is given by σ then the symmetry of the reverse pulse is given by $(1-\sigma)$.

Table 3 gives the calculated results for peak heights and half widths for various square wave amplitudes and symmetries. For this table, both the first and second scans have the same symmetry, therefore for an asymmetric square wave the reverse pulse has a different length than the forward pulse. Of particular note is that the peak width can be considerably decreased by making the waveform asymmetric. This is in contrast to regular rapid scan

square wave in which the peak width at half height is fairly independent of the symmetry of the square wave. Also not only are the peaks narrower for small σ's, but the amount of diminution is less.

At first glance, a short forward pulse for the first sweep combined with a short reverse pulse for the second sweep would seem like the best combination. Although this choice of symmetry relationship gives the largest response, it also gives the broadest peaks. The two peaks, although larger, are too far apart to give a reasonable response. The best symmetry relationship is one where one current is large and the other is fairly small. The choice of square wave amplitude is also important as large square amplitudes show considerable broadening.

Figure 13 shows the theoretical forward, reverse and difference currents for the alternate drop mode as well as the difference current for regular square wave. The alternate drop mode shows a marked broadening of the peak and is diminished. The reason for the broadening and diminution arises from the same problem that DPR mode has, mainly that the reverse current has been shifted toward the initial potential by 2 E_{sw} and this is sufficient to invalidate the additive nature of the difference measurement.

Figure 14 gives an example of the use of this technique at the trace level. Although difficult to see with this figure, the square wave alternate drop mode does reduce the amount of background. Since relatively small square wave amplitudes must be used in order to keep the peak width at a reasonable value, this mode does not do as well as the differential pulse modes.

It is obvious that a good deal more work can be done for the square wave mode. While not all possible variations in parameters have been studied, it was thought that the values chosen had the best chance of

being the optimum. Perhaps variations in measurement times and symmetry relationships can maximize this mode.

As is the case for the alternate drop modes of Christie et al, potential dependent adsorption of trace organics of any kind can invalidate the assumption that the capacity current is independent of the previous history of the waveform. In the case of adsorption, the capacity background may be incompletely compensated by these techniques.

Up until recently, all electroanalytical techniques at the dropping mercury electrode had a charging current contribution due to the growing drop. With the advent of the techniques proposed here and the ones developed by Christie et al (1,2,3), this charging current background has been eliminated. Not all the problems with trace analysis at the dme have been dealt with, but at least headway is being made.

Although no alternate drop technique has yet been applied to a "real" sample, it is hoped that with the introduction of commercial instrumentation these techniques and others yet to be developed will find use in pulse polarographic methodology.

TABLE 1

Comparison of ordinary and alternate drop differential pulse forward mode.

n E_{dp}	Ratio δ/τ	Ordinary Peak Height	Ordinary Peak Width	Alternate Drop Peak Height	Alternate Drop Peak Width	Diminution Factor
mV			mV		mV	%
15	.5	.216	90.1	.100	99.1	46.3
25	.5	.377	91.9	.166	100.5	44.0
65	.5	.934	104.0	.394	112.4	42.2
85	.5	1.14	113.6	.482	122.0	42.2
15	.33	.251	90.6	.164	97.8	65.3
25	.33	.426	92.2	.271	99.2	63.6
65	.33	1.03	104.3	.643	111.1	62.4
85	.33	1.25	114.1	.786	120.8	62.3
15	.25	.287	90.8	.211	97.0	73.5
25	.25	.481	92.4	.347	98.4	72.1
65	.25	1.15	104.5	.822	110.4	71.5
85	.25	1.40	114.2	1.00	120.0	71.4

$n\Delta E$ = 5 mV

TABLE 2

Comparison of ordinary and alternate drop differential pulse reverse mode.

E_{dp}	Ratio δ/τ	Ordinary Peak Height	Ordinary Peak Width	Alternate Drop Peak Height	Alternate Drop Peak Width	Diminution Factor
mV			mV		mV	%
10	.5	- .199	92.5	-.067	98.7	33.7
20	.5	- .361	93.1	-.133	99.8	36.8
60	.5	- .925	103.8	-.369	110.4	39.9
80	.5	-1.14	113.2	-.461	119.4	40.4
10	.33	- .198	91.9	-.107	97.5	54.0
20	.33	- .373	92.6	-.212	98.5	56.8
60	.33	- .984	103.3	-.585	109.2	59.5
80	.33	-1.21	112.6	-.731	118.3	60.4
10	.25	- .214	91.6	-.141	96.6	65.9
20	.25	- .411	92.4	-.280	97.6	68.2
60	.25	-1.10	103.1	-.771	108.3	70.1
80	.25	-1.36	112.3	-.962	117.4	70.7

$n\Delta E = 5$ mV

TABLE 3

Comparison of ordinary and alternate drop square wave

$n E_{sw}$	σ	Ordinary		Alternate drop		Diminution Factor
		Peak Height	Peak Width	Peak Height	Peak Width	
mV			mV		mV	%
10	.5	.361	93.1	.288	105.2	79.8
20	.5	.664	97.0	.482	112.0	72.6
30	.5	.925	103.8	.607	147.3	65.6
50	.5	1.30	124.8	.721	213.8	55.4
10	.33	.409	93.5	.340	102.3	83.1
20	.33	.735	97.5	.574	113.9	78.1
30	.33	1.02	104.4	.751	129.3	73.6
50	.33	1.24	113.8	.981	163.0	69.0
10	.25	.464	93.6	.395	100.5	85.6
20	.25	.825	97.7	.676	109.2	82.0
30	.25	1.14	104.7	.899	120.5	78.9
50	.25	1.39	114.1	1.21	145.8	76.6

Conditions: $n\Delta E = 5$ mV, $\rho_1 = \sigma - 0.001$, $\rho_2 = 0.999$

ACKNOWLEDGMENT

The homemade potentiostat and I-E converter used for some of this work was built by Chaim Yarnitzky.

CREDIT

This work was supported by the National Science Foundation under Grant CHE-75-00332, and by the Office of Naval Research under Contract N00014-77-C-0004.

LITERATURE CITED

1. J. H. Christie, Ph.D. Thesis, Colorado State University, Fort Collins, Colorado, 1974.

2. J. H. Christie, L. L. Jackson and R. A. Osteryoung, Anal. Chem., 48, 242 (1976).

3. J. H. Christie, L. L. Jackson and R. A. Osteryoung, Anal. Chem., 48, 561 (1976).

4. J. H. Christie, R. A. Osteryoung, J. Electroanal. Chem., 49, 301 (1974).

5. J. H. Christie, J. A. Turner and R. A. Osteryoung, Anal. Chem., 49, 000 (1977).

6. J. A. Turner, J. H. Christie, M. Vukovic and R. A. Osteryoung, Anal. Chem., 49, 000 (1977).

7. J. A. Turner, Ph.D. Thesis, Colorado State University, Fort Collins, Colorado, 1977.

8. T. Kambara, Bull. Chem. Soc. Japan, 27, 523 (1954).

9. S. C. Rifkin and D. H. Evans, Anal. Chem., 48, 1616 (1976).

10. G. C. Barker and A. W. Gardner, AERE Harwell, C/R 2297 (1958).

11. G. C. Barker, Anal. Chim. Acta, 18, 118 (1958).

FIGURE CAPTIONS

FIGURE 1: Potential-time profile and timing for rapid scan alternate drop normal pulse polarography.
Solid line = waveform for first drop
Dashed line = waveform for second drop

FIGURE 2: Current-potential characteristics for rapid scan alternate drop normal pulse polarography. 8.42×10^{-5} M Cd in 0.1 M HCl. Conditions: ΔE = 5 mV; τ(NP) = 33.3 msec; δ(NP) = 16.7 msec; τ(SC) = 50 msec; T_d = 1 sec; Ave = 10; m = .785 mg/sec. Instrument PAR 174. Currents normalized to delay time.

FIGURE 3: Rapid scan normal pulse polarograms of 8.43×10^{-7} M Cd in 0.1 Cd in 0.1 M KCl. (a) ordinary (b) alternate drop. Conditions: ΔE = 5 mV; τ = 37.5 msec; σ = 12.5 msec; τ(SC) = 50 msec; T_d = 2 sec; Ave = 30. Instrument = 48 J. Currents normalized to delay time.

FIGURE 4: Potential-Time Profile and Timing for Rapid Scan Alternate Drop Constant Potential Pulse Polarography.
Solid line first scanning waveform.
Dashed line second "waveform".

FIGURE 5: Current-potential characteristics for rapid scan alternate drop constant potential pulse polarography. A. 8.42×10^{-5} M Cd in 0.1 M HCl. ΔE = 5 mV; τ = 16.7 msec; δ = 16.7 msec; T_d = 2 sec; Ave = 10; Instrument PAR 174. (B) 8.42×10^{-7} M Cd in 0.1 M KCl. ΔE = 5 mV; τ = 37.5 msec; δ = 12.5 msec; T_d = 2 sec; Ave = 30; Instrument 48 J. m = .785 mg/sec. Currents have been inverted for this figure and normalized to delay time.

FIGURE 6: Potential-time profile and timing for rapid scan alternate drop differential pulse forward mode.
Solid line = waveform for first scan
Dashed line = waveform for second scan.

FIGURE 7: Current potential characteristics for rapid scan alternate drop differential pulse forward mode. 8.42×10^{-5} M Cd in 0.1 M HCl. A. Difference Current. B. Individual Pulse and Staircase Currents. Conditions: For difference and pulse measurement - E_{dp} = 35 mV; τ = 37.5 msec; δ = 12.5 msec; ΔE = 5 mV; T_d = 1 sec; Ave = 15. For staircase measurement - ΔE = 5 mV; τ = 50 msec; T_d = 1 sec; Ave = 10; m = .785 mg/sec. Instrument PAR 174.

FIGURE 8: Comparison of rapid scan differential pulse and rapid scan alternate drop differential pulse forward mode for 2×10^{-7} M lead in 0.1 F KCl. (a) ordinary (b) alternate drop. Conditions: E_{dp} = 90 mV; τ = 50 msec; δ = 16.7 msec; T_d = 1 sec; ΔE = 5 mV; m = .785 mg/sec. Instrument 48J. Currents normalized to delay time.

FIGURE 9: Potential-time profile and timing for rapid scan alternate drop differential pulse reverse mode.
Solid line = waveform for first scan
Dashed line = waveform for second scan.

FIGURE 10: Theoretical individual pulse and staircase currents for differential pulse reverse mode. Conditions: ΔE = 5 mV; E_{dp} = 60 mV; ratio (δ/τ) = .25.

FIGURE 11: Rapid scan alternate drop differential pulse reverse mode polarogram for 2×10^{-7} M lead in 0.1 M KCl. Conditions same

as Figure 8. Currents have been inverted for this figure and normalized to the delay time.

FIGURE 12: Potential-time profile and timing for rapid scan alternate drop square wave polarography.

Symmetry of forward pulse waveform (solid line) = .2

Symmetry of reverse pulse waveform (dashed line) = .8

FIGURE 13: Theoretical currents for regular and alternate drop rapid scan square wave. A. Difference current (-) ordinary, (...) alternate drop. B. Individual forward and reverse currents for alternate drop. Conditions: $n\Delta E$ = 5 mV; n E_{sw} = 30 mV; σ = .33.

FIGURE 14: Comparison of ordinary and alternate drop rapid scan square wave polarography for 2 x 10^{-7} M lead in -.1 F KCl. (a) ordinary, (b) alternate drop. Conditions: E_{sw} = 20 mV; ΔE = 5 mV; σ = .33; τ = 50 msec; m = .785 mg/sec. Instrument 48J. Currents normalized to delay time.

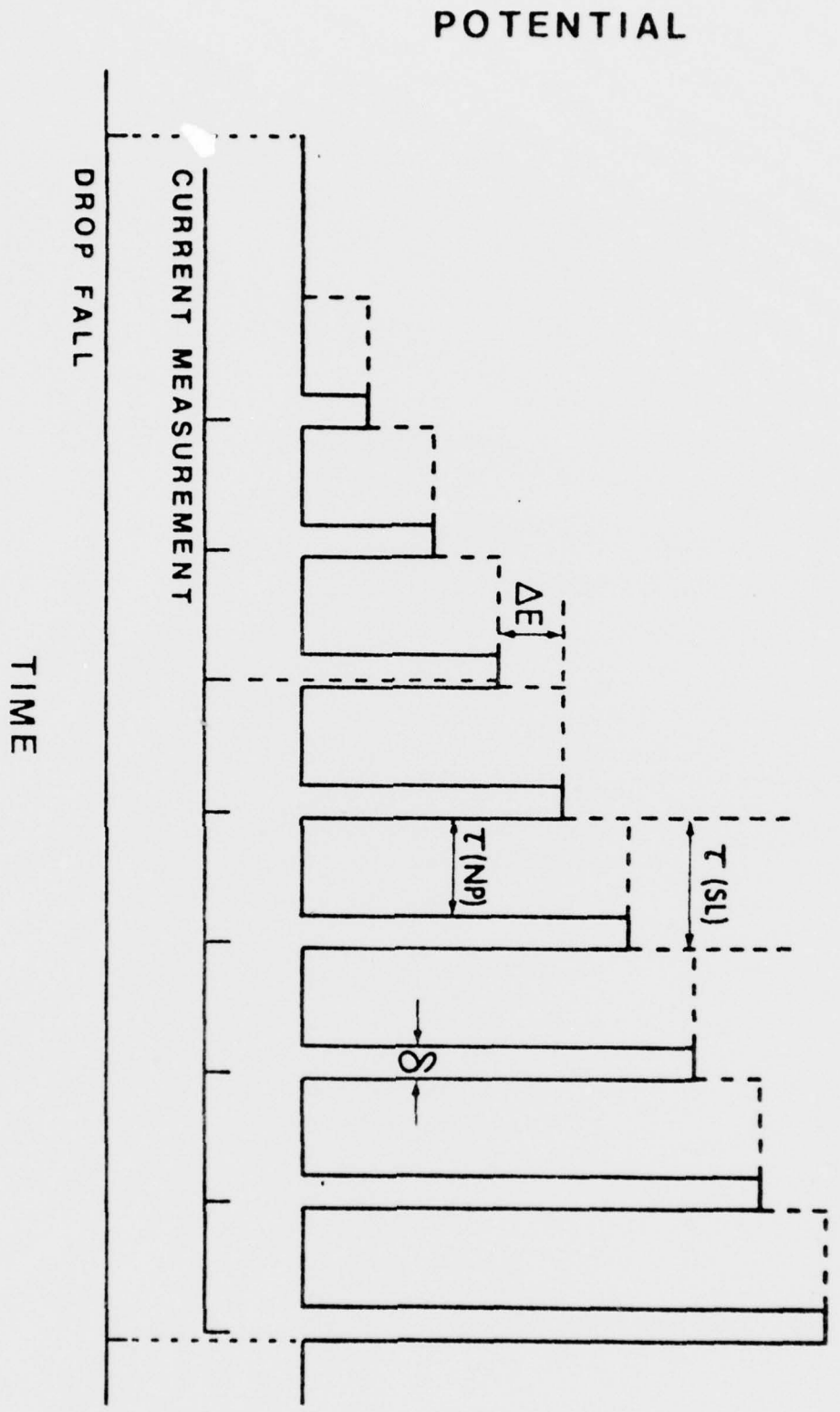

FIGURE 1

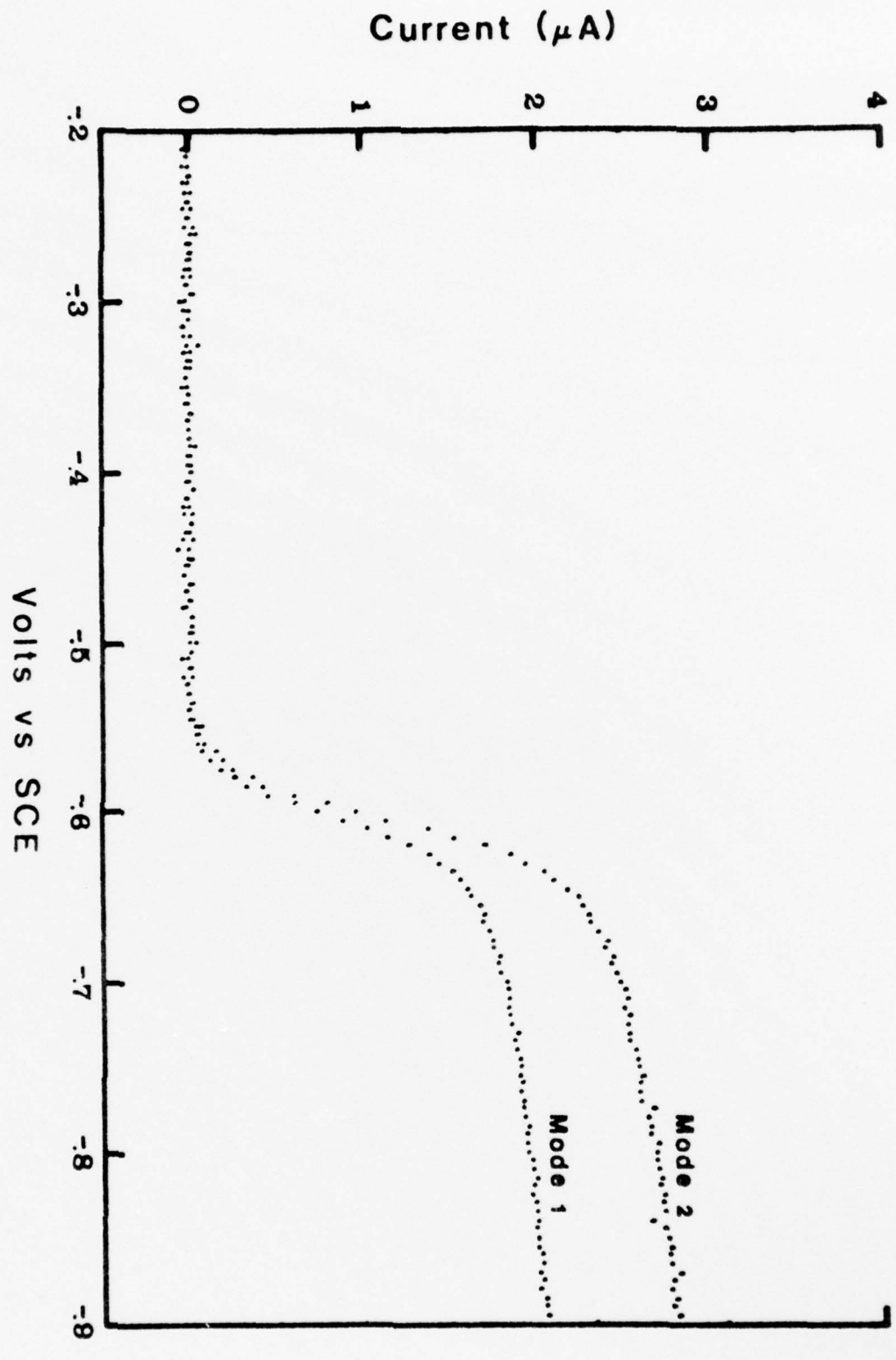

FIGURE 2

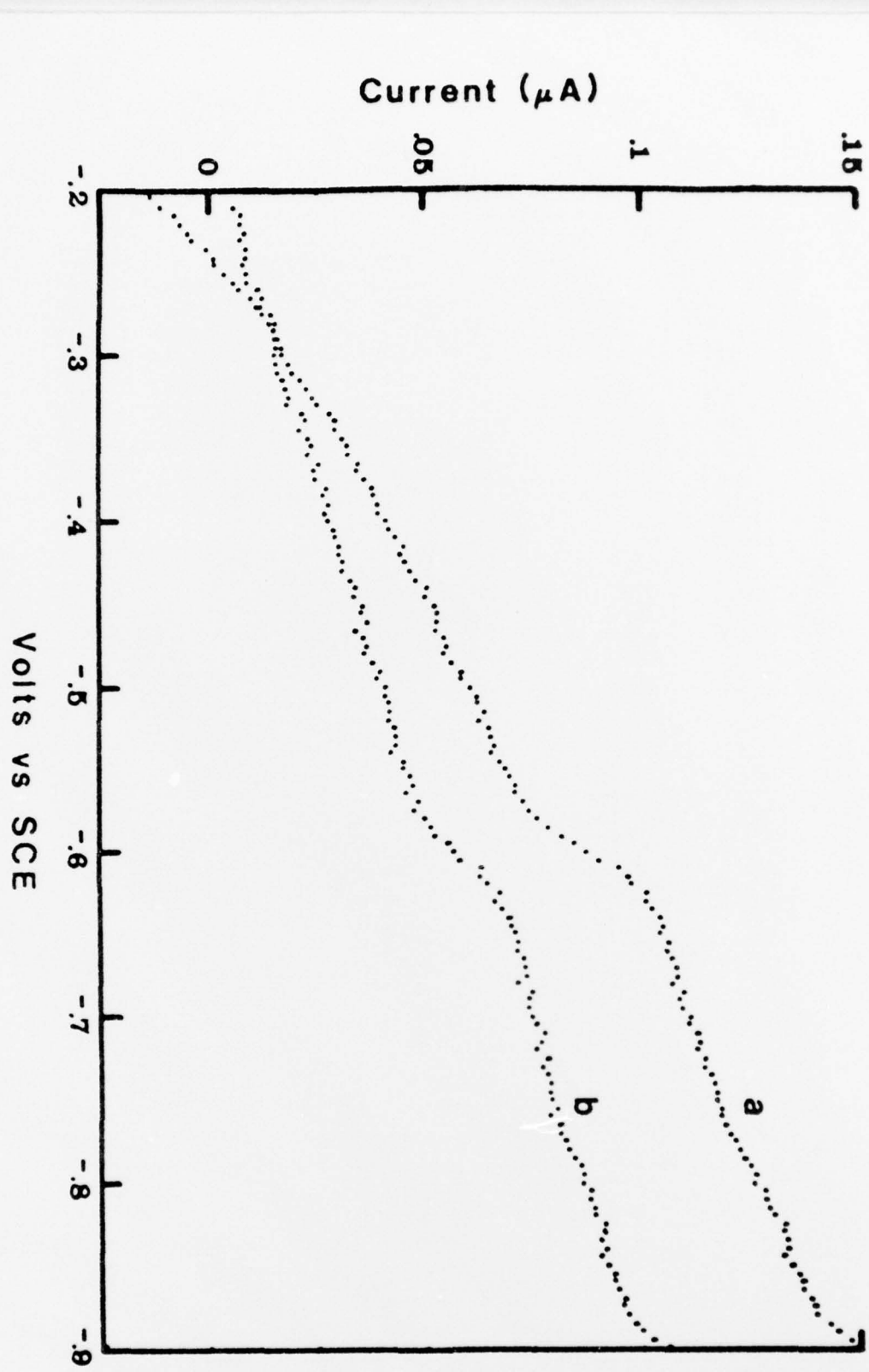

FIGURE 3

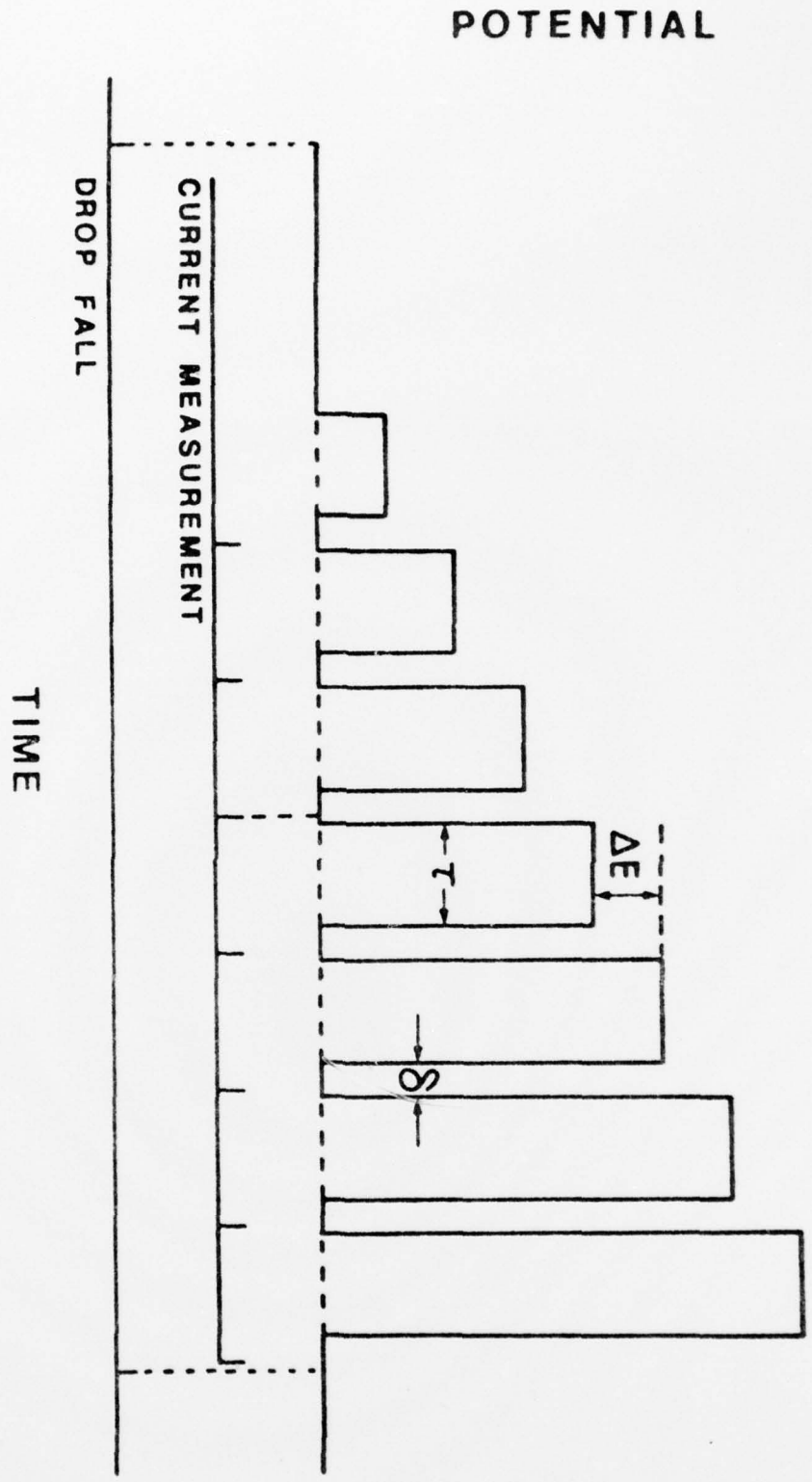

FIGURE 4

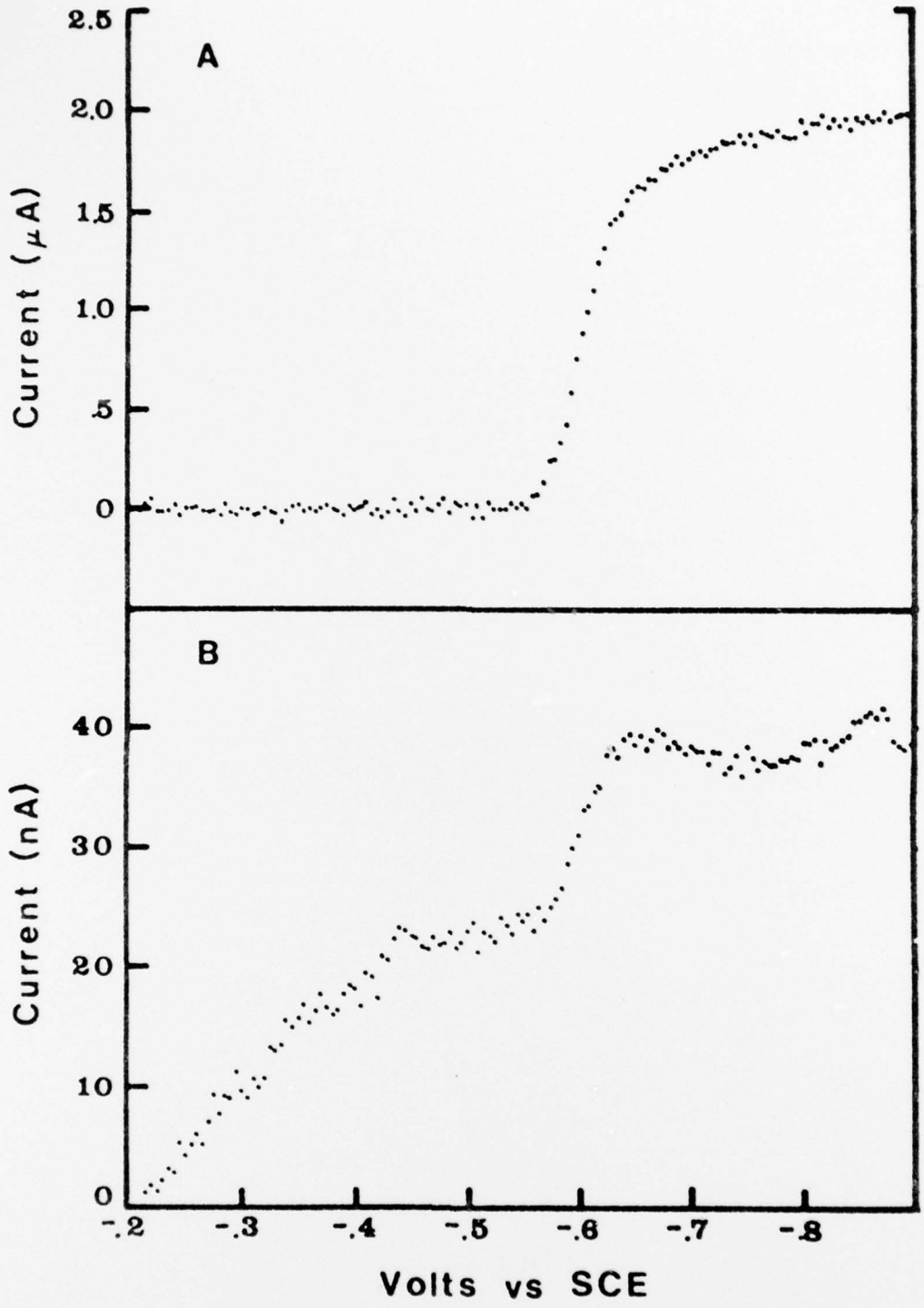
A
B
Current (μA)
Current (nA)
2.5
2.0
1.5
1.0
.5
0
40
30
20
10
0
-.2
-.3
-.4
-.5
-.6
-.7
-.8
Volts vs SCE

FIGURE 5

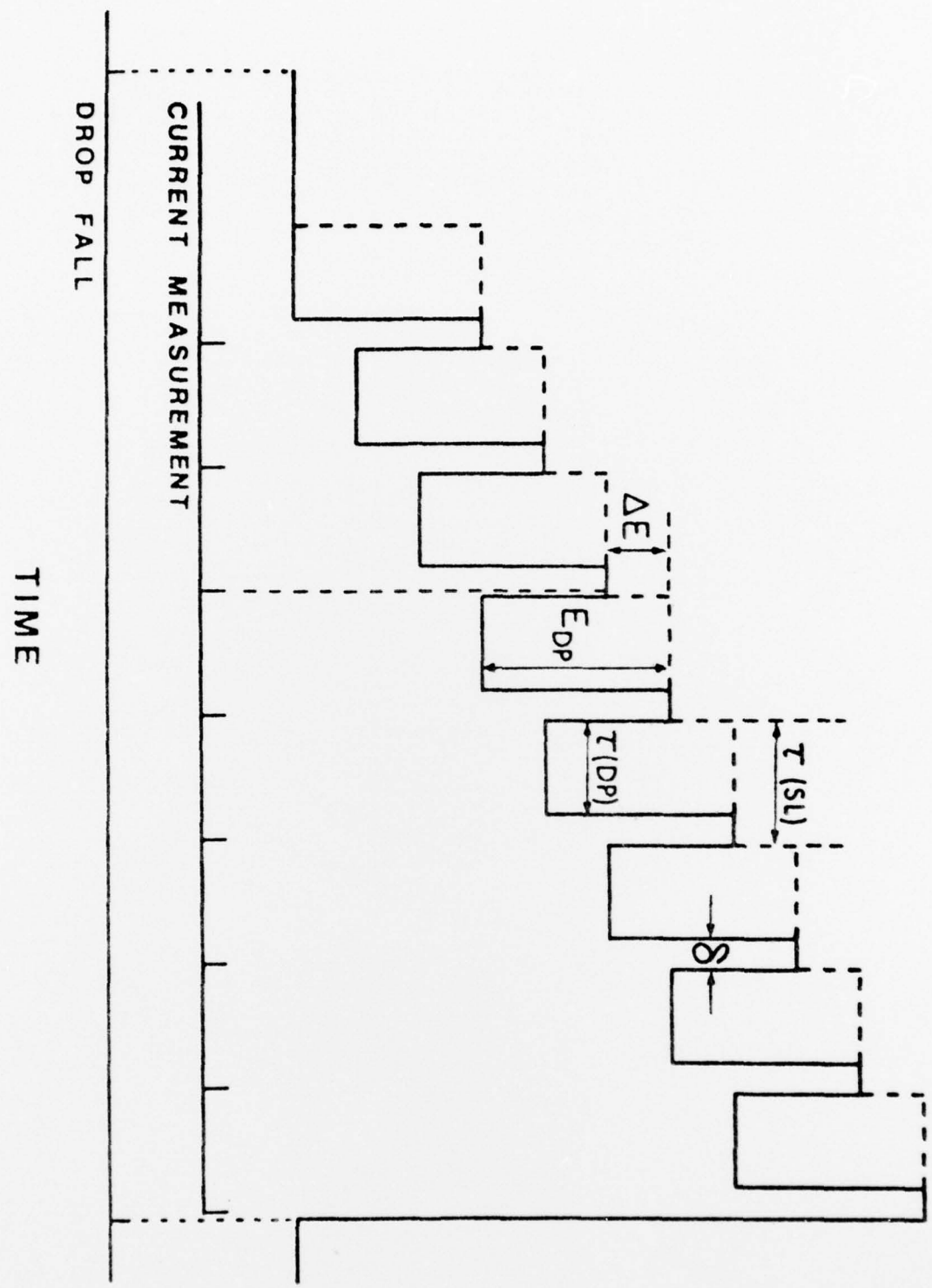
POTENTIAL
DROP FALL
CURRENT MEASUREMENT
TIME
ΔE
E_{DP}
$\tau_{(DP)}$
$\tau_{(SL)}$
δ

FIGURE 6

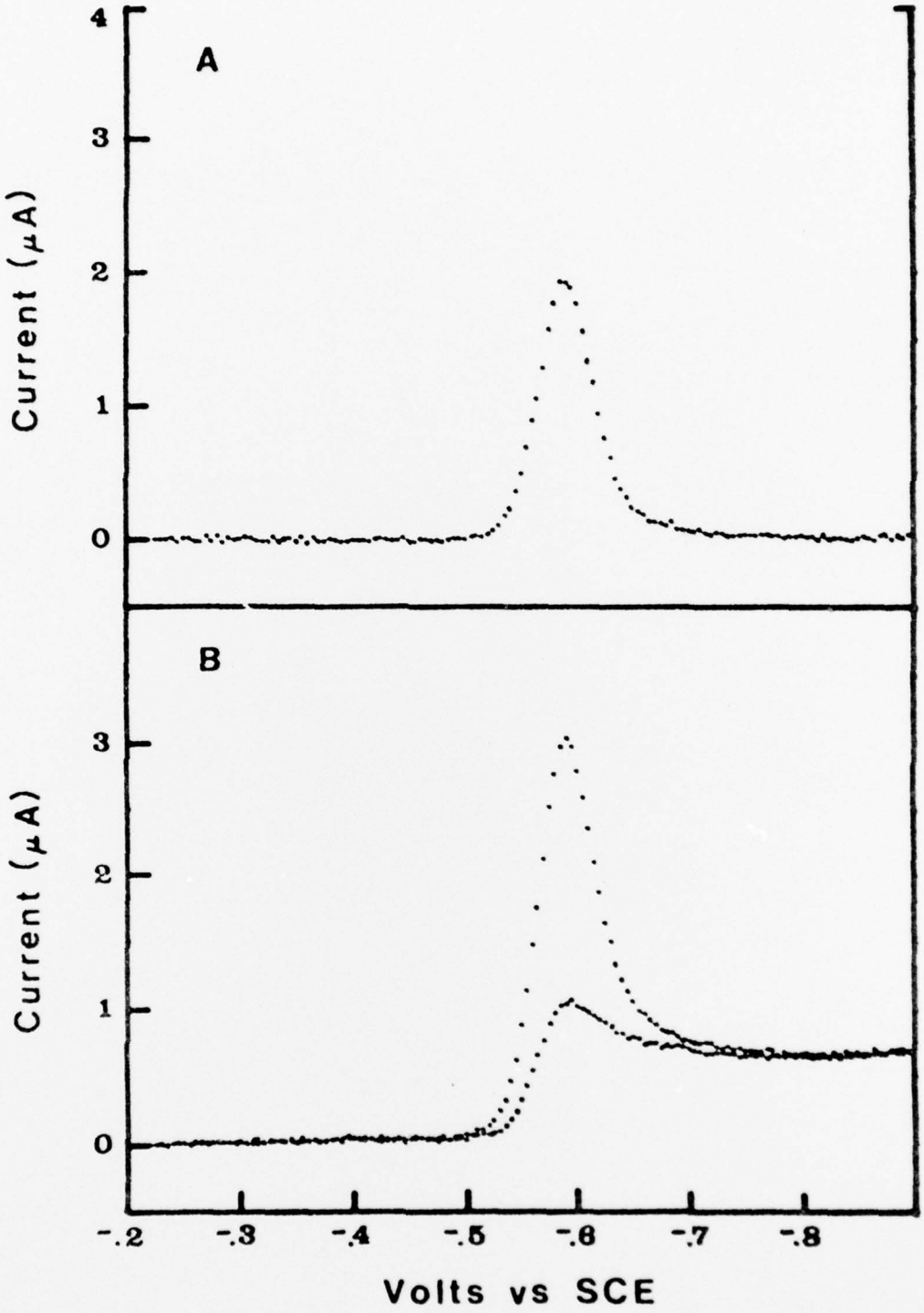

FIGURE 7

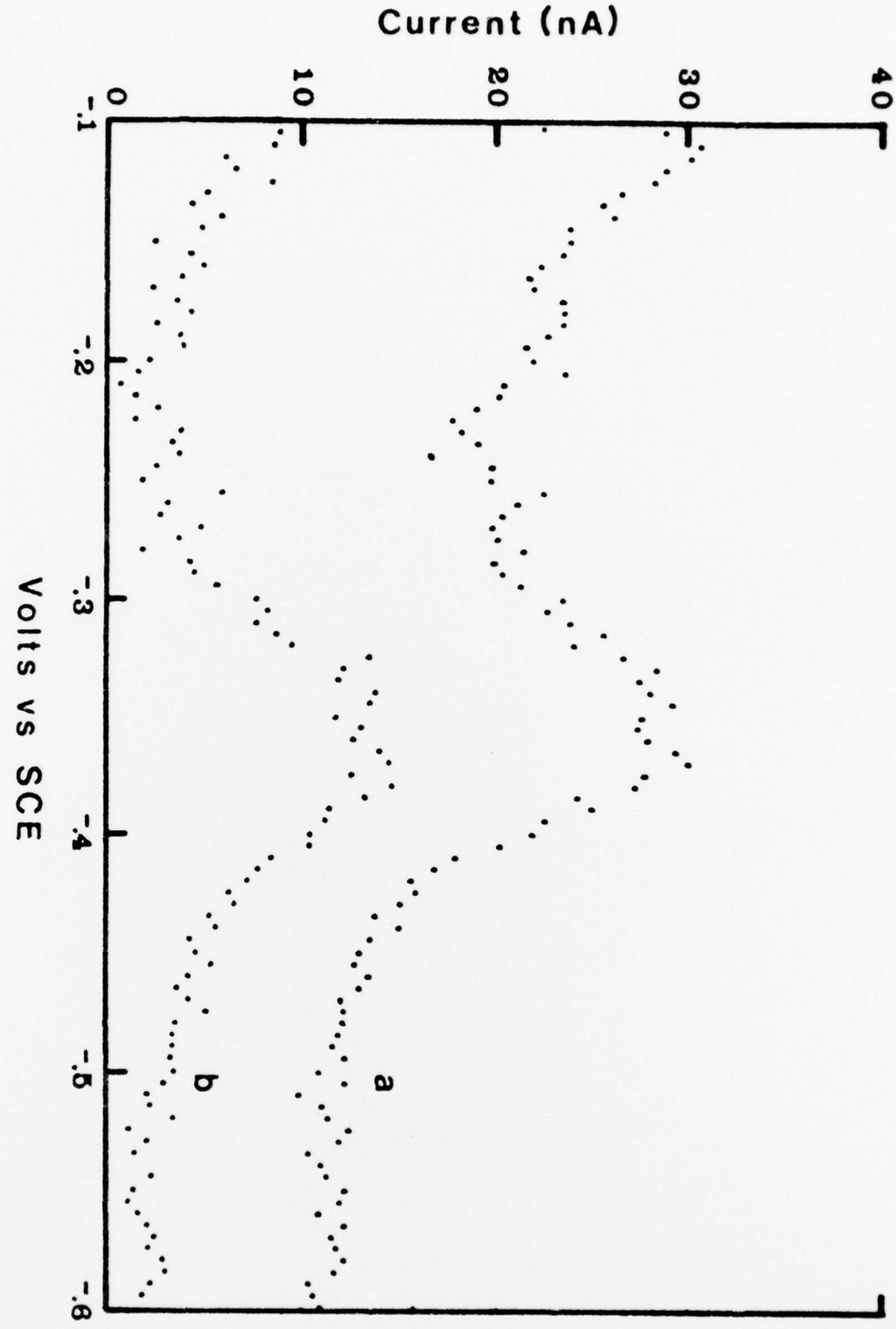

FIGURE 8

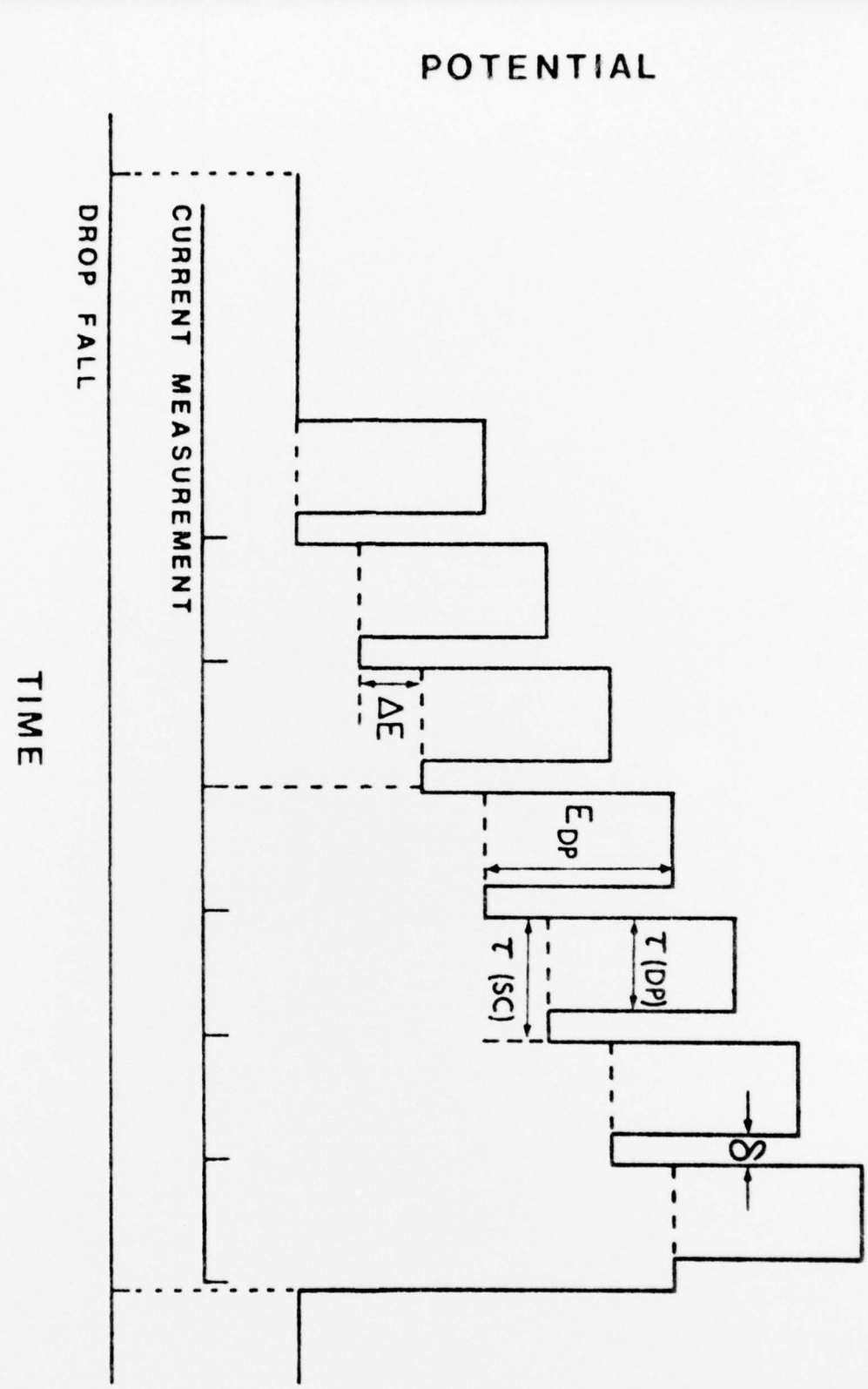
POTENTIAL
DROP FALL
CURRENT MEASUREMENT
TIME
ΔE
E_DP
τ (SC)
τ (DP)
δ

FIGURE 9

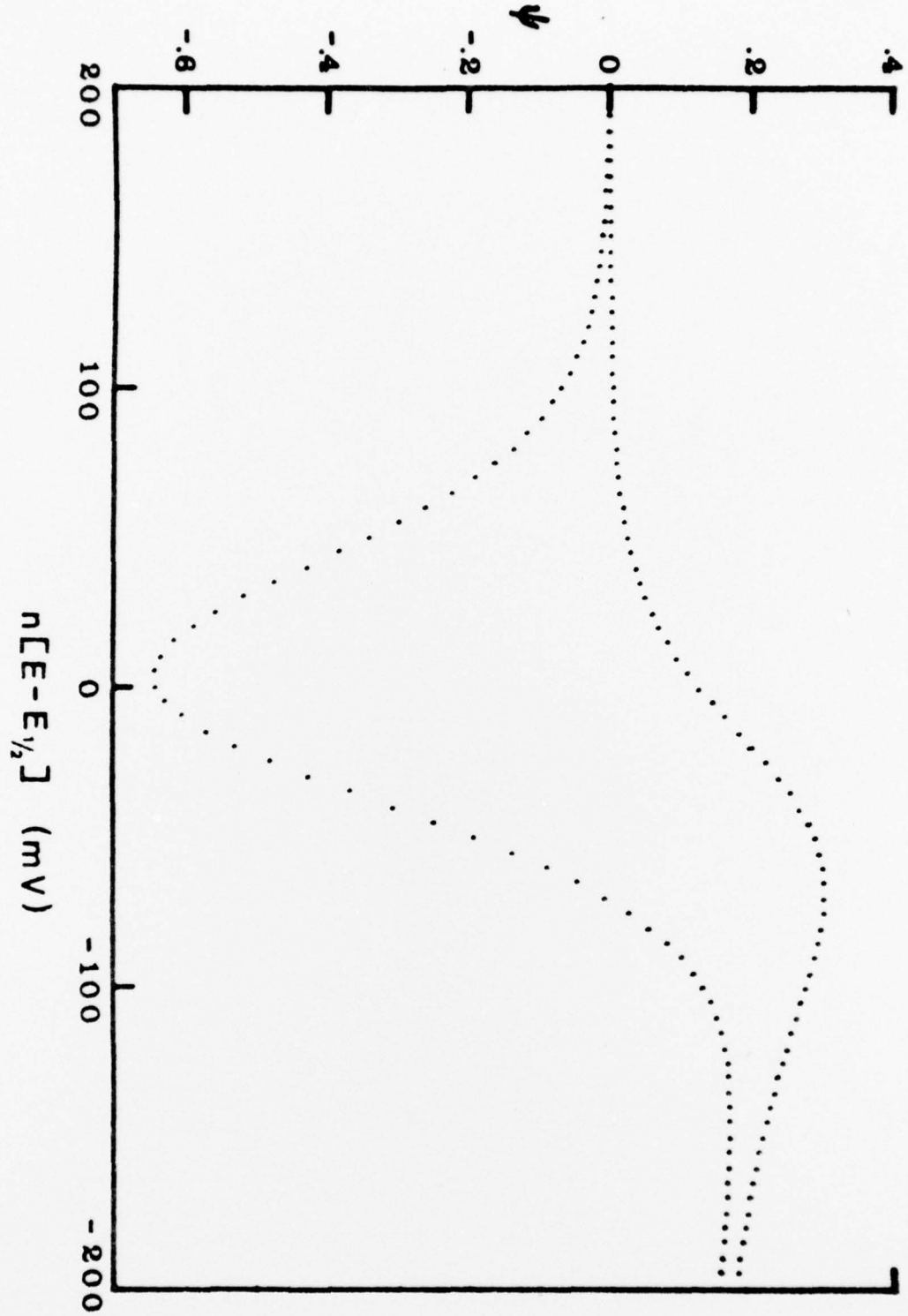

FIGURE 10

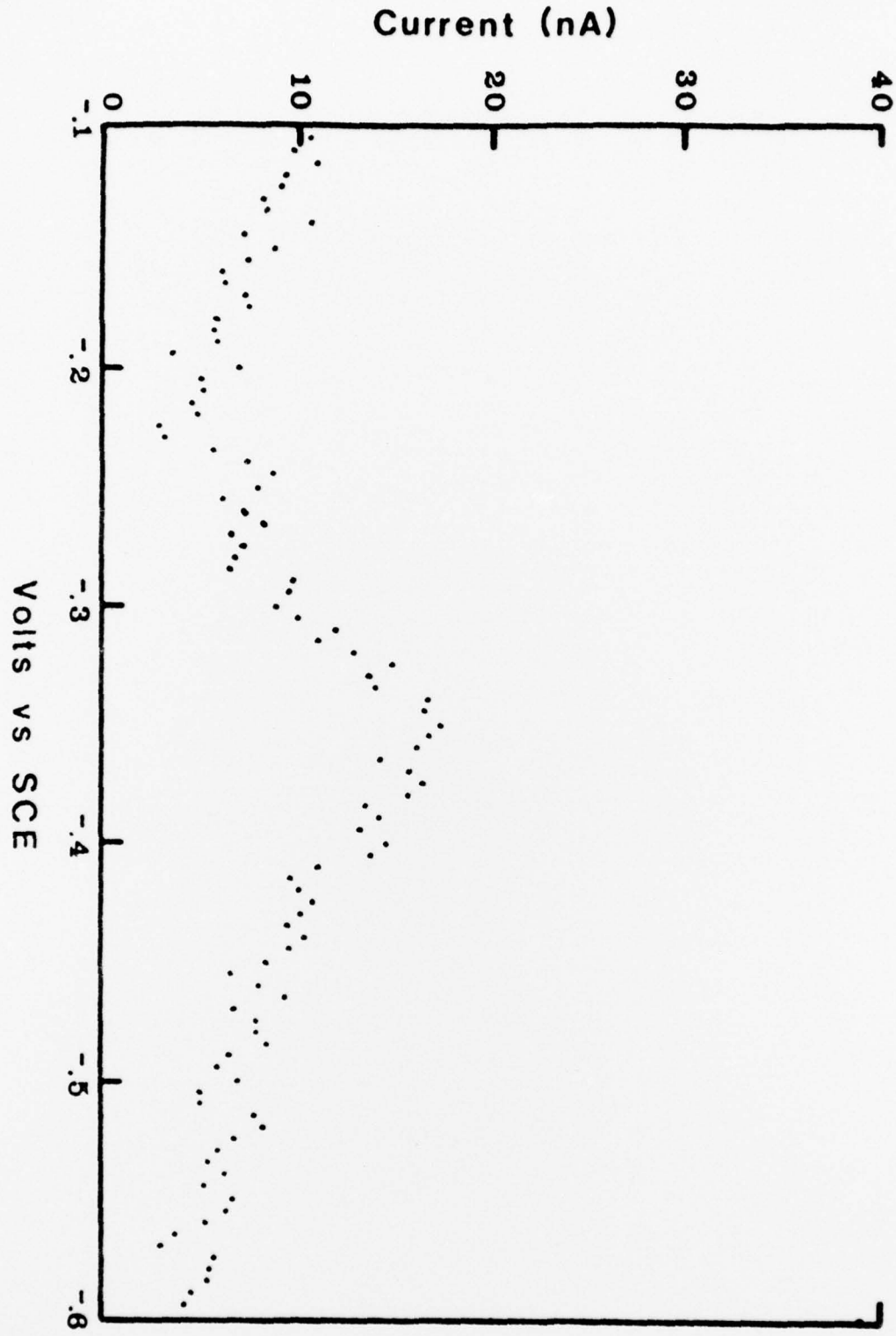

FIGURE 11

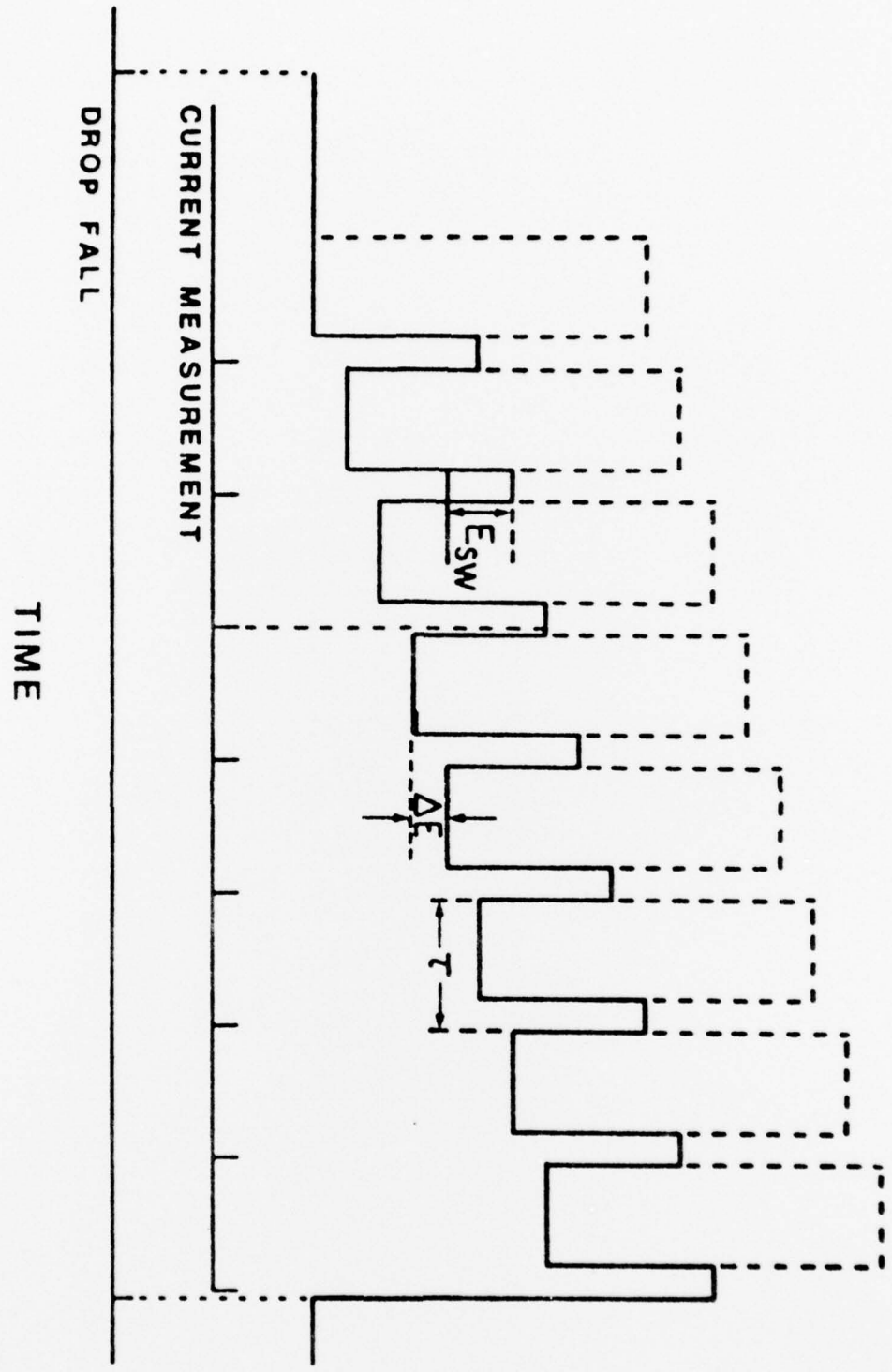
POTENTIAL
DROP FALL
CURRENT MEASUREMENT
TIME
E_{SW}
ΔE
τ

FIGURE 12

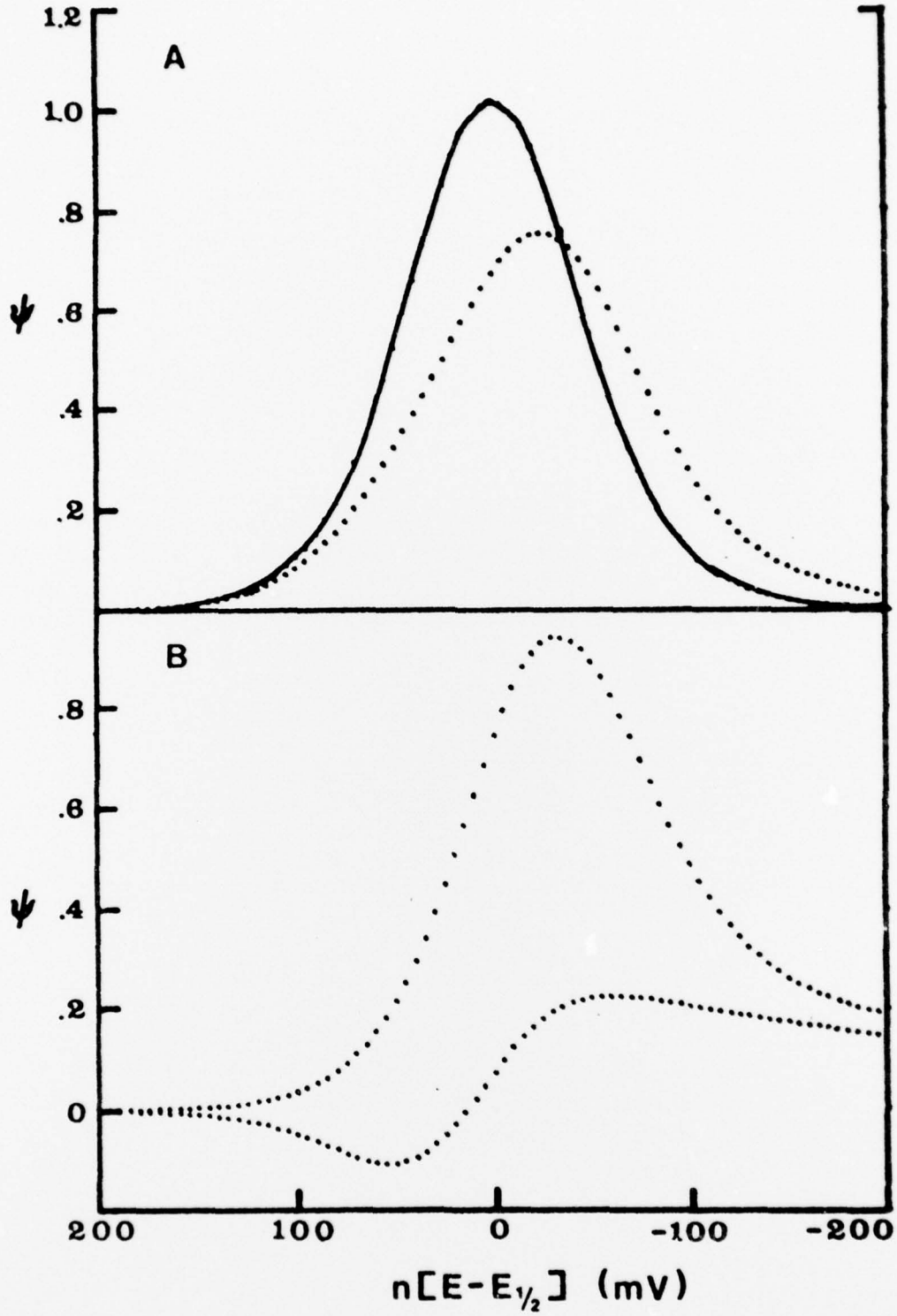

FIGURE 13

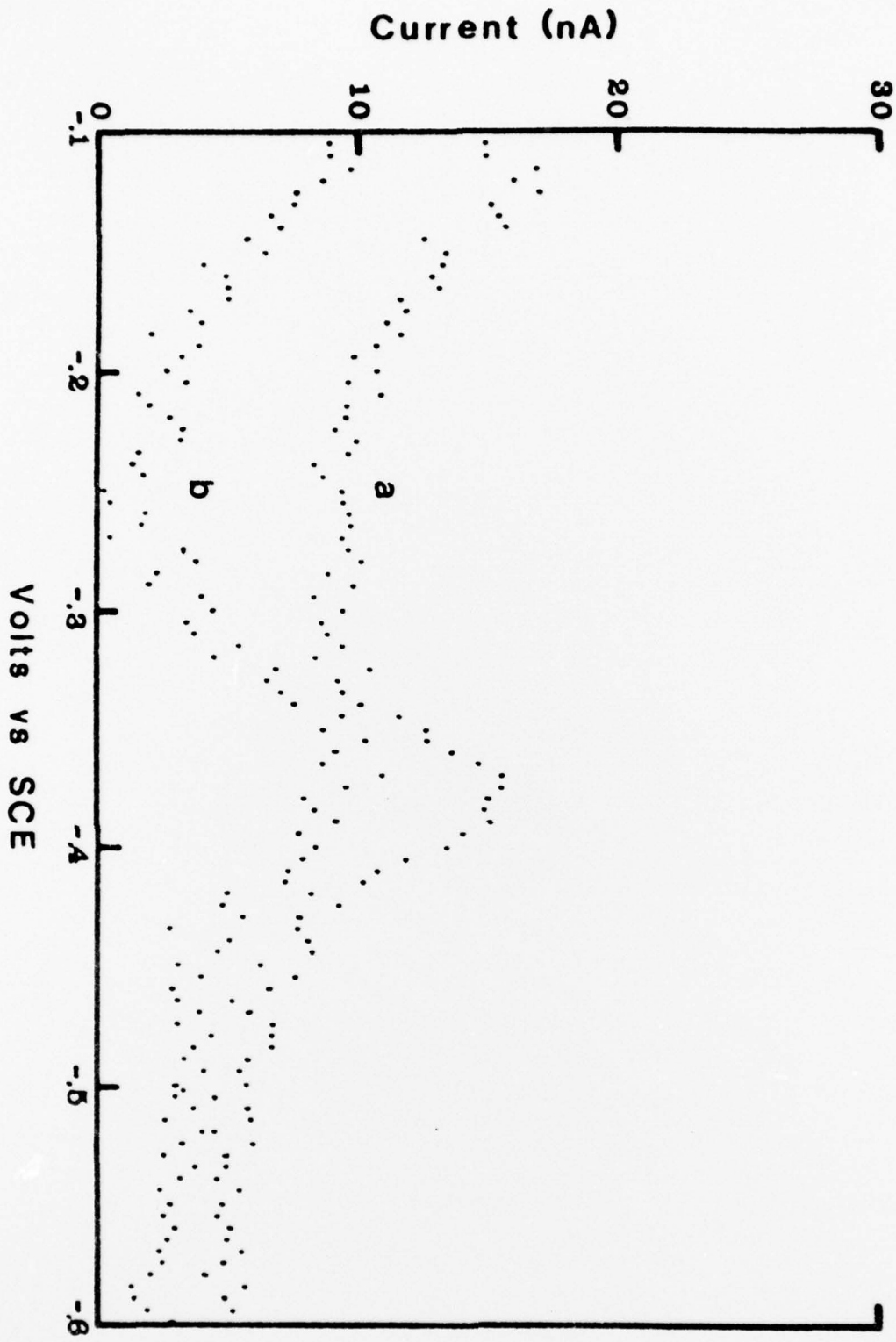

FIGURE 14

TECHNICAL REPORT DISTRIBUTION LIST

	No. Copies
M. B. Denton versity of Arizona artment of Chemistry son, Arizona 85721	1
G. S. Wilson versity of Arizona artment of Chemistry son, Arizona 85721	1
R. A. Osteryoung orado State University artment of Chemistry Collins, Colorado 80521	1
B. R. Kowalski versity of Washington artment of Chemistry ttle, Washington 98105	1
I. B. Goldberg h American Rockwell Science Center Box 1085 Camino Dos Rios sand Oaks, California 91360	1
S. P. Perone ue University rtment of Chemistry yette, Indiana 47907	1
E. E. Wells l Research Laboratory 6160 ington, D.C. 20375	1
D. L. Venezky l Research Laboratory 6130 ington, D.C. 20375	1
d. Freiser ersity of Arizona tment of Chemistry n, Arizona 85721	

	No. Copies
Dr. Fred Saalfeld Naval Research Laboratory Code 6110 Washington, D.C. 20375	1
Dr. H. Chernoff Massachusetts Institute of Technology Department of Mathematics Cambridge, Massachusetts 02139	1
Dr. K. Wilson University of California, San Diego Department of Chemistry La Jolla, California 92037	1
Dr. A. Zirino Naval Undersea Center San Diego, California 92132	1
Dr. John Duffin United States Naval Post Graduate School Monterey, California 93940	1
Dr. G. M. Hieftje Department of Chemistry Indiana University Bloomington, Indiana 47401	1
Dr. Victor L. Rehn Naval Weapons Center Code 3813 China Lake, California 93555	1
Dr. Christie G. Enke Michigan State University Department of Chemistry East Lansing, Michigan 48824	1

TECHNICAL REPORT DISTRIBUTION LIST

	No. Copies
fice of Naval Research lington, Virginia 22217 tn: Code 472	2
fice of Naval Research lington, Virginia 22217 tn: Code 102IP 1	6
Branch Office S. Clark Street cago, Illinois 60605 n: Dr. Jerry Smith	1
Branch Office Broadway York, New York 10003 n: Scientific Dept.	1
Branch Office 0 East Green Street adena, California 91106 n: Dr. R. J. Marcus	1
Branch Office Market Street, Rm. 447 Francisco, California 94102 n: Dr. P. A. Miller	1
Branch Office Summer Street ton, Massachusetts 02210 n: Dr. L. H. Peebles	1
ctor, Naval Research Laboratory ington, D.C. 20390 n: Code 6100	1
Asst. Secretary of the Navy (R&D) rtment of the Navy 4E736, Pentagon ington, D.C. 20350	1
ander, Naval Air Systems Command rtment of the Navy ington, D.C. 20360 n: Code 310C (H. Rosenwasser)	1

	No. Copies
Defense Documentation Center Building 5, Cameron Station Alexandria, Virginia 22314	12
U.S. Army Research Office P.O. Box 12211 Research Triangle Park, N.C. 27709 Attn: CRD-AA-IP	1
Naval Ocean Systems Center San Diego, California 92152 Attn: Mr. Joe McCartney	1
Naval Weapons Center China Lake, California 93555 Attn: Head, Chemistry Division	1
Naval Civil Engineering Laboratory Port Hueneme, California 93041 Attn: Mr. W. S. Haynes	1
Professor O. Heinz Department of Physics & Chemistry Naval Postgraduate School Monterey, California 93940	1
Dr. A. L. Slafkosky Scientific Advisor Commandant of the Marine Corps (Code RD-1) Washington, D.C. 20380	1
Office of Naval Research Arlington, Virginia 22217 Attn: Dr. Richard S. Miller	1